Journal of Integrative Neuroscience, Vol. 8, No. 1 (2009) 77-93
© Imperial College Press

Imperial College Press
www.icpress.co.uk

Research Report

RECEPTIVE FIELD SIZES OF DIRECTION-SELECTIVE UNITS IN THE FISH TECTUM

ILIJA DAMJANOVIĆ*, ELENA MAXIMOVA
and VADIM MAXIMOV

Institute for Information Transmission Problems
Russian Academy of Sciences, Bolshoi Karetny 19
127994 Moscow, Russia
* damjanov@iitp.ru

Received 4 December 2008
Accepted 3 February 2009

Responses of direction-selective (DS) ganglion cells (GCs) were recorded extracellularly from their axon terminals in the superficial layer of tectum opticum (TO) of immobilized cyprinid fish *Carassius gibelio* (Bloch, 1782). Excitatory receptive field (ERF) sizes of six types of DS GCs (ON and OFF cells, each of three distinct preferred directions) were evaluated on the basis of four different methods. In Method 1, the ERF width was calculated as a product of duration of spike train, generated in response to contrast edge moving across the ERF in preferred direction, and the velocity of the stimulus movement. The duration of spike train was estimated either as an interval between the first and the last spikes, or on the basis of the width of bell-shaped post-stimulus histogram of spike response according to its standard deviation. More precise size and position of the ERF can be outlined with edges moving in many different directions. So, in Method 2 diameter of the ERF was calculated on the basis of a mean distance of position of spike appearance from the center of ERF. Method 3 — ERF tracing by small contrast spot moving on several parallel tracks allowed estimation of the ERF width by number of spikes along each track and the ERF length by the duration of spike train. When tracing in two mutually orthogonal projections, the method also permitted calculation of the value of the temporal delay in the network from the same experiment. Canonical method (Method 4) used the ERF mapping with contrast spots flickering sequentially in different places of stimulation area. The length, width and orientation of the ERF were evaluated according to the two-dimensional equivalent of the standard deviation for this data set. All applied methods gave consistent estimates of ERF sizes — mean values of ERF sizes for all four procedures ranged between 4° and 4.8°. These angle values corresponded to retinal area of approximately 300 μm. Small ERFs of the fish DS GCs measured in the current study, indicate that the fish DS units should be classified as "fast" DS units, and are most likely involved in the detection of small objects moving in the surrounding environment.

Keywords: Direction-selective ganglion cells; excitatory receptive field; tectum opticum; *Carassius gibelio.*

*Corresponding author.

1. Introduction

Ganglion cells (GCs) represent the final information processing system in the vertebrate retina. An entire visual scene is encoded by many GCs, whose receptive fields (RFs) are distributed over the image plane at the retinal surface. RFs of ganglion cells are usually functionally divided into central and peripheral parts. Presentation of an adequate stimulus in the central part of RF evokes response from the cell. On the other hand, no response is obtained if only the RF periphery is stimulated. The responsive or excitatory central part of the RF (ERF) corresponds to the area covered by cell dendritic arborization, which allows GC to collect visual signals over relatively broad visual space. In the rabbit retina it was shown that ERFs and the areas covered by dendritic arbors of GCs are similar in size [27, 28].

Information about different properties of visual objects: size, direction of motion, form, color, etc. is processed by different types of specialized GCs (detectors). The detectors have been described in the fish retina also [4, 8, 9, 12, 17, 24, 29]. The information processed by the specialized GCs is transmitted to primary visual centers of the fish brain, mainly midbrain formation *tectum opticum* (TO). When a microelectrode is perpendicularly advanced through the fish TO layers, the responses from different GC projections in TO can be recorded. In superficial layers of TO, responses of direction-selective (DS) units are constantly recorded. These detectors respond to the stimuli moving in a particular (preferred) direction and give no response to the stimuli moving in the opposite or null direction. In recent studies [18, 19] it was shown that DS GCs in the Prussian carp[a] are divided into three distinct groups, characterized by the preferred movement directions: caudo-rostral, ventro-dorsal, and dorso-ventral, separated by about 120°. In each group the DS GCs are represented by ON and OFF cell subtypes in relatively equal amount. The fact that the number of DS GC groups in the species corresponds to the number of semicircular canals, implies that the fish DS GCs projecting to the TO may be involved in some multimodal sensory integration in postural, locomotor and oculomotor control in the 3D aquatic world [18, 19]. In this respect, fish DS GCs projecting to the TO resemble the rabbit "slow" DS GCs projecting to the nuclei of the accessory optic system [21]. However, the rabbit "slow" DS GCs are represented only by the ON cell subtype. Those ON GCs comprise three physiological groups according to the directions they prefer, similar to the DS GCs in the fish. The rabbit ON GCs respond to slow movements and are characterized by large receptive fields — two features typical for detectors analyzing the global motion. On the other hand, detectors of local motion in the rabbit retina (so called "fast" DS GCs that prefer one of the four different directions and belong to the ON-OFF subtype) are characterized by relatively small RFs, which are more than three times smaller than those in the "slow" ON units [23].

[a] The Prussian carp used to be regarded either as a subspecies of the goldfish (*Carassius auratus)* or as its wild form, but is now considered as an independent species — *Carassius gibelio.*

The aim of the current study is to define more precisely the physiological function of the fish DS GCs on the basis of their ERF sizes. Consequently, the detailed measurement of the ERF sizes of the fish ON and OFF DS units will be accomplished. As DS GCs are characterized by the complex structure of their RFs which are non-concentric in the sense of Kuffler [11], various stimulating procedures may affect the response originating in the ERF in different ways [3]. Thus in our study, ERF sizes of the fish DS GCs were estimated using different types of the visual stimuli: contrast edges moving across the ERF, small contrast spot moving across the ERF, and, finally, flickering spot (canonical stimulus for ERFs mapping). The combined data, obtained from these different procedures, can give us additional information about the size and the structure of complex DS GCs RFs.

2. Material and Methods

2.1. *Experimental animals*

The data were collected from the *Carassius gibelio* (Bloch, 1782), 10 to 15 cm in length (snout to tail) and weighing 35 to 100 g each. Fishes were acquired from local suppliers (Moscow region) and maintained during several months in aerated fresh water aquaria, at room temperature (18-22°C) and natural daylight regime.

2.2. *Preparation*

During the experiments the animals were immobilized (d-tubocurarine, *i.m.)*. The dosage of tubocurarine (0.3 mg/100 g) was adjusted so as to induce the arrest of eyes and respiratory movements. The fish were placed in their natural position in a transparent Plexiglas tank where artificial respiration was provided continuously by forcing aerated water through the gills. In order to reveal TO contra-lateral to the stimulated eye, an opening was made in the skull over the contra-lateral midbrain. During the surgery the preparation site of the head was anesthetized with ice. Dura and pia mater were dissected and excess of fatty tissue and fluid were aspirated. The water level in experimental tank was kept constant, the eyes being under the water. The animals were decapitated after the experiment, and their brain and eyes were used for histological explorations.

2.3. *Visual stimulation*

Visual stimuli (contrast edges and spots moving with various speeds in different directions) were presented on the computer-controlled CRT monitor to the right eye of the fish through the transparent tank wall. The lateral visual fields, covering the area of more than 60° in width and about 40° in height, were investigated. Distance between the 17 inch monitor screen and the fish eye during the experiments was about 30 cm. When calculating the angular size of the stimuli the refraction of the rays on the front wall of the aquarium was taken into account. Preliminary

estimates of ERFs sizes [19] determined the stimulation area as a square with side of approximately 11° on the monitor screen (45° × 35°). Constant luminosity was maintained on the rest of the monitor surface.

2.4. *Data acquisition*

Responses of DS GCs were recorded extracellulary in the superficial layers of the TO. Low impedance (200-500 KΩ) microelectrodes were made using micropipettes filled with a Wood's metal and tipped with a platinum cap of 2-10 μm in diameter [7]. The microelectrode was guided to a necessary tectal area under the visual control by means of micromanipulator according to the retinotopic projection [8]. The microelectrode was carefully advanced through the superficial layers until stable single-unit response was recorded. The main criteria characterizing the single-unit response were the high and stable spike amplitude and the high signal/noise ratio. The responses gained in an AC preamplifier (band pass 100 Hz to 3.5 kHz), were listened in a loudspeaker, monitored on an oscilloscope and digitized by an A/D converter (25 kHz sampling rate). Responses, loaded into the computer during the registration interval, were stored: (a) without former processing (for subsequent analysis of spike form) or (b) after filtering according to amplitude discrimination. They were stored as a sequence of moments of the spike appearance for further analysis.

2.5. *Computer modules*

Three mutually connected and synchronized computer modules were used during the experimental work: (a) the recording module, connected to the microelectrode through the A/D and the preamplifier; it served for recording of the neuron responses, further visualization of the responses on the screen and, finally, stores the experimental data; (b) stimulating module controls the stimulating monitor on which various visual stimuli were presented to the fish; (c) controlling module, which served for additional online graphic demonstration of the processed data and for operative manipulation by stimulation and recording parameters during the experiment. For the controlling module a special interface was designed, allowing the investigator to change efficiently the parameters of the program designed for experiment control. The standard experimental procedures such as the polar diagram measurement, estimation of the ERF sizes (and so on) were designed in the form of the program tools described elsewhere [19].

2.6. *Polar diagram measurement*

All experimental procedures, performed for ERF size estimation, were preceded by the measurement of cell polar diagram. Examples of the polar diagrams measured for three different units are shown in Figs. 1(A), 3(A) and 5(A) (the preferred

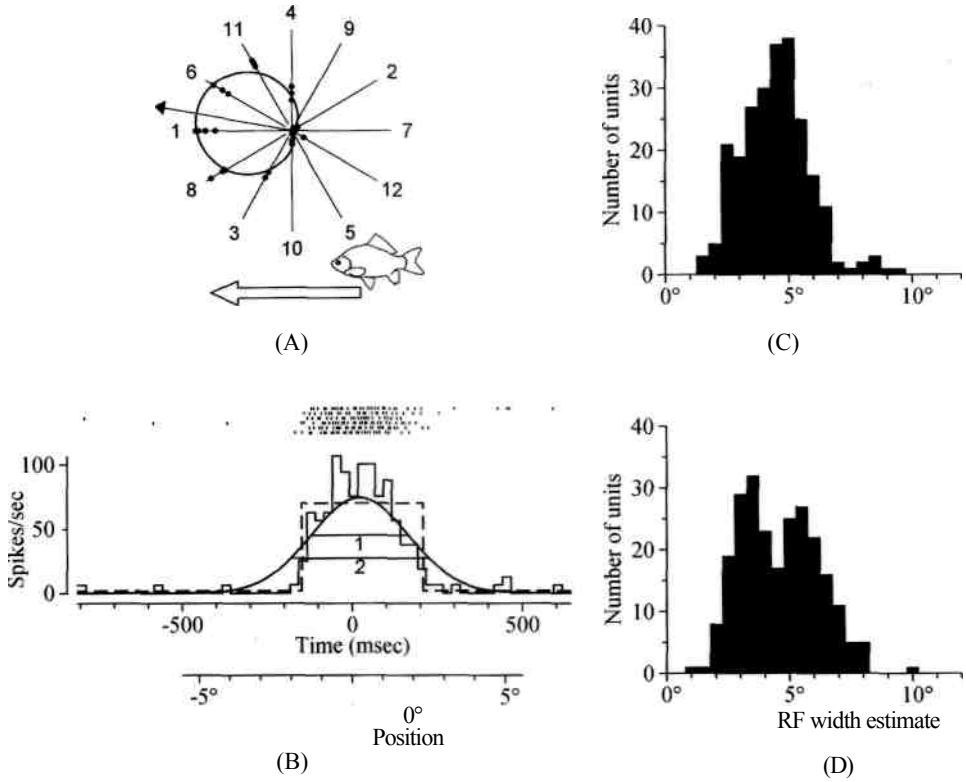

Fig. 1. Evaluation of the ERF size from the duration of spike train evoked by contrast edge moving in the preferred direction across stimulation area (Method 1). (A) An example of polar diagram of an ON DS unit selective to caudo-rostral movement. Responses to light edges moving in 12 directions at a speed of 11°/sec against a dark background are presented in the diagram. The figures at the end-points of radii designate an order of measurements for different directions of movement. Dots mark the number of spikes evoked in response to each of three runs for each applied directions. Solid curve represents approximation of experimental data by a second order harmonic function. Preferred direction of the cell is shown by a black arrow. An ERF size was evaluated by this method on the basis of the response evoked by contrast edge moving across the ERF in the direction closest to the preferred one; this direction is shown by an open arrow at the bottom of Fig. 1(A). (B) *Top panel:* moments of spike appearance during the stimulation, plotted as dots against the time scale; *bottom panel:* stepped solid curve is a post-stimulus histogram of the discharge, showing the number of evoked spikes along the time or position scales; stepped dashed curve describes the discharge by means of maximal likelihood method; bell-shaped curve represents Gaussian function drawn according to Eq. (3.1). Horizontal chords of the Gaussian curve represent its width at the levels (1) 0.607 and (2) 0.368 of maximum (detailed explanation in the text). *The time scale:* zero point corresponds to the moment of stimulus leading edge passing through the center of stimulation area. *The position scale (in "degrees"):* zero point corresponds to the position of center of stimulation area; rostro-caudal direction is positive. The scale enables fixing of the position of stimulus leading edge on the monitor surface at the moment of spike appearance. An ERF size can be determined from the position scale. (C) Histogram of distribution of the ERF sizes in 241 DS GCs, calculated from standard deviation. (D) Histogram of distribution of the ERF sizes, calculated by means of maximal likelihood method.

directions of cells are marked by black arrows). Responses to the contrast edges moving in 12 different directions over the neutral (gray) background are presented in the diagrams. Three stimulus trials were usually applied for each direction. Black dots represent number of spikes evoked by each of the three trials for every direction used. Solid lines represent the approximation of the experimental data by a second order harmonic function. At the end of the procedure a measurement for the first direction was repeated in order to check the unit response level.

3. Results

ERF sizes of the fish DS GCs were evaluated on the basis of four different methods.

3.1. *Determination of ERF size from the cell response to contrast edge moving in the preferred direction (Method 1)*

The sizes of the ERF were evaluated from the cell responses to the contrast edges moving in directions close to the preferred ones for each of the three groups of DS cells studied (caudo-rostral, dorso-ventral, ventro-dorsal). Rough estimate of the ERF width can be calculated as a product of the duration of the spike train (discharge) and the velocity of the stimulus movement.

For this purpose, we used several hundreds of polar diagrams for DS GCs accumulated in the database. For each diagram from all directions of movement of the contrast edge, the one that was nearest to the preferred direction was chosen. An example of such a polar diagram is shown in Fig. 1(A). The preferred direction, calculated by the phase of the first harmonic of the Fourier transform, is shown by the black arrow. The nearest measured direction for this diagram was caudo-rostral one, which was used in the first and final sessions of the measurement. At the top panel of Fig. 1(B) moments of spike appearance in all six trials in this direction are plotted as dots against the time scale. The same data can be considered as positions x of stimulus leading edge in the stimulation area at the moment t of spike appearance: $x = v \cdot t$, where v is the velocity of edge movement. Corresponding position scale is shown at the bottom of Fig. 1(B).

Duration of the spike discharge (or its width in the spatial scale) was determined by the post-stimulus histogram (PSH) in two ways. First, the length of the discharge can be outlined from the temporal (spatial) dispersion of spikes in the train. For this purpose we calculated: (a) the position of the ERF center as a mean position of spikes in the discharge $\bar{x} = \frac{1}{N}\sum_x N_x \cdot x$; and (b) standard deviation for the PSH $\sigma = \sqrt{\frac{1}{N}\sum_x N_x \cdot (x - \bar{x})^2}$, where x is a position of stimulus leading edge, N_x is the number of spikes in position x, and N is total number of spikes in the discharge. The PSH for the cell presented in Fig. 1 is shown by a solid stepped curve at the bottom panel of Fig. 1(B), while a bell-shaped curve represents a Gaussian model [6] of the ERF (density of spikes in the position x, G_x) with the defined values of

the mean *($\bar{x}$)* and standard deviation *(σ)* calculated according to the equation:

$$G_x = \frac{N}{\sigma \cdot \sqrt{2\pi}} \cdot e^{\frac{-(x-\bar{x})^2}{2\sigma^2}} . \tag{3.1}$$

An estimation of the ERF width directly as the doubled standard deviation (which corresponds to the width of the Gaussian curve at the level of 0.607 of maximum) looks underestimated (see chord 1 in Fig. 1(B)). The width of the Gaussian at the level l/e = 0.368 of maximum (chord 2) seems intuitively to be more plausible. In this case the ERF size, *D,* according to this method is equal to:

$$D = 2 \cdot \sqrt{2} \cdot \sigma . \tag{3.2}$$

The histogram of the ERF sizes distribution for 241 DS GCs (including 119 ON units and 123 OFF units of all preferred directions) estimated with this procedure is presented in Fig. 1(C). The ERF sizes varied from 2 to 10°, with the mean value of 4.7 ± 1.4°. Significant differences in the ERF sizes, either between ON and OFF units, or between DS GCs preferring different directions, were not observed.

Second, to verify the validity of the ERF size using Eq. (3.2), an additional statistical estimation procedure was carried out. Duration of the response was defined as the time interval between the first and the last spike in the train evoked by the stimulus. On the basis of the response duration and the velocity of the stimulus movement, it was possible to calculate diameter of the ERF. However, sparse incidental spikes superimposed on the response can complicate an automatic procedure of such a measurement of the response duration. In order to filter the evoked spikes from incidental and spontaneous ones, generated before and after the evoked train, a statistical model of maximum likelihood function was designed. It was supposed that the sequence of spikes in the record was a result of two random processes: (a) the process of high probability of spike generation during the train, evoked by the stimulus moving across the cell ERF, and (b) the process with low probability of spike generation, reflecting spontaneous activity of the cell before and after the train. The corresponding likelihood function depends on the probability values mentioned above and moments of time which define the beginning (t_1) and the end (t_2) of a train.

The aim of the procedure was to maximize the likelihood function, by varying the set of parameters, and finally define the values t_1 and t_2. Then, the difference $t_2 - t_1$ was multiplied by the velocity of the stimulus motion and the obtained result was considered as an estimate of the ERF size for the analyzed unit (Fig. 1(B), stepped dashed curve).

The histogram of the ERF sizes distribution for the same group of 241 DS GCs estimated by this procedure is presented in Fig. 1(D). The ERF sizes varied from 2 to 8°, with the mean value of 4.8 ± 1.6°. Significant differences in ERF sizes, either between ON and OFF units, or between DS GCs preferring different directions, were not observed. Thus, the ERF diameter obtained with maximum likelihood

procedure is close to the mean ERF size estimated on the basis of the standard deviation procedure.

3.2. *Determination of RF size and position by contrast edge moving in different directions (Method 2)*

Size and position of the ERF can be outlined more precisely from cell responses to the contrast edge moving in many different directions. Experimental data used by this method were the same as in Method 1, namely, polar diagrams for DS GCs. The ERF sizes were evaluated from the sequences of moments of spike appearances in all trials for all directions of movement on the basis of the following offline procedure. The center of the ERF was determined as a point in the visual field, where mean square deviation of the moment of spike appearance from the moment of stimulus passing through the ERF center was minimal. The obtained value of the root mean square deviation was used instead of standard deviation σ in Eq. (3.2) to get an estimate of the ERF size.

Unfortunately, the moments of spike registration may be delayed in time relative to the moments of edge passing through the RF because of synaptic latencies in the retinal network. As a result, when moving stimuli at high speed, some spikes appear after the edge has already left the stimulation area. There are two ways to overcome this disadvantage: (1) not to use high speed stimulus for measurements of the ERF sizes; and (2) determine the value of delay and take it into account. We have used both ways. One way to determine the delay is described below in Method 3. There the network delays were calculated for 77 DS units. The mean delay was approximately 50 ms.

Figure 2(A) illustrates an application of Method 2 in determining the ERF size for the same ON caudo-rostral DS unit whose polar diagram is shown in Fig. 1(A). Positions of leading edge of the stimulus at the moment of spike appearance (taking into account the temporal delay of 50 ms) are marked by thin black lines inside the stimulation area for all directions applied. A circle located in the area of maximal density of the crossed lines indicates the position and the size of the ERF calculated by Method 2.

The histogram of the ERF size distribution for 252 DS GCs (ON and OFF units presented in equal quantities) represented in Fig. 2(B) was evaluated by this method, taking into account the 50 ms delay. The mean value of the ERF diameter, calculated for all cells made 4.4 ± 1.3°. Significant differences in ERF sizes, either between ON and OFF units, or between DS GCs preferring different directions were not observed, similar as in Method 1.

3.3. *Determination of RF size and position by RF tracing with moving spots (Method 3)*

Tracing of ERF by small contrast spot moving along several parallel tracks allow estimation of ERF size and position. When the ERF tracing is accomplished in

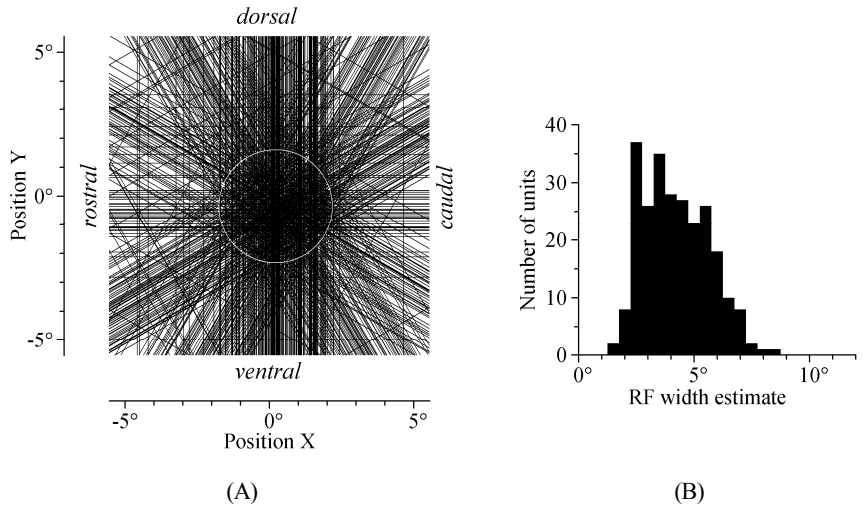

(A) (B)

Fig. 2. Evaluation of the ERF size by contrast edges moving in 12 different directions across the stimulation area (Method 2). (A) Responses to light edges, moving in 12 directions against dark background across the receptive field of the same DS unit as in Fig. 1; every black line corresponds to the position of the moving edge at the moment of spike appearance, assuming a temporal delay in the retinal network of 50 ms; circle in the central part of stimulation area represents the estimated ERF area. (B) Histogram showing distribution of the ERF sizes in 252 DS GCs, calculated by Method 2 with consideration of 50 ms network temporal delay.

two mutually orthogonal directions, the value of the network temporal delay may be calculated in the same experiment. Light spots against dark background and dark spots against light background were used as stimuli for ON and OFF units, correspondingly. Figure 3 illustrates the method. The ERF tracing of an ON DS unit with preferred ventro-dorsal direction was performed (polar diagram of this unit is shown in Fig. 3(A)). Velocity of the spot movement was 16.5°/sec. The tracing was accomplished along nine parallel tracks in each of the two mutually orthogonal directions, marked by open arrows in Fig. 3(A). Three stimulus trials were applied for each of the nine tracks. Positions of the spot leading edges in the moments of spike appearance are marked by dashes inside the stimulation area (top of Fig. 3(B)). Number of spikes, evoked along each track, was calculated for both of the traced directions. The corresponding columns in bar histograms represent the number of spikes calculated along the ERF for each direction. The spot movements along two marginal tracks evoked no response in this experiment (marginal tracks for the right histogram are marked by thin interrupted lines in Fig. 3(B)). The position of the ERF center and σ-values can be determined from the first and the second moments of the histograms. In Fig. 3(B), dashed Gaussian curves were calculated from these values for both directions. The ERF extensions can be estimated for each of the directions separately, on the basis of calculated standard deviations σ_1 and σ_2 according to the Eq. (3.2). An equivalent diameter of the ERF was considered to be equal to the geometric mean of these values: $\overline{D} = \sqrt{D_1 \cdot D_2}$. The ERF size

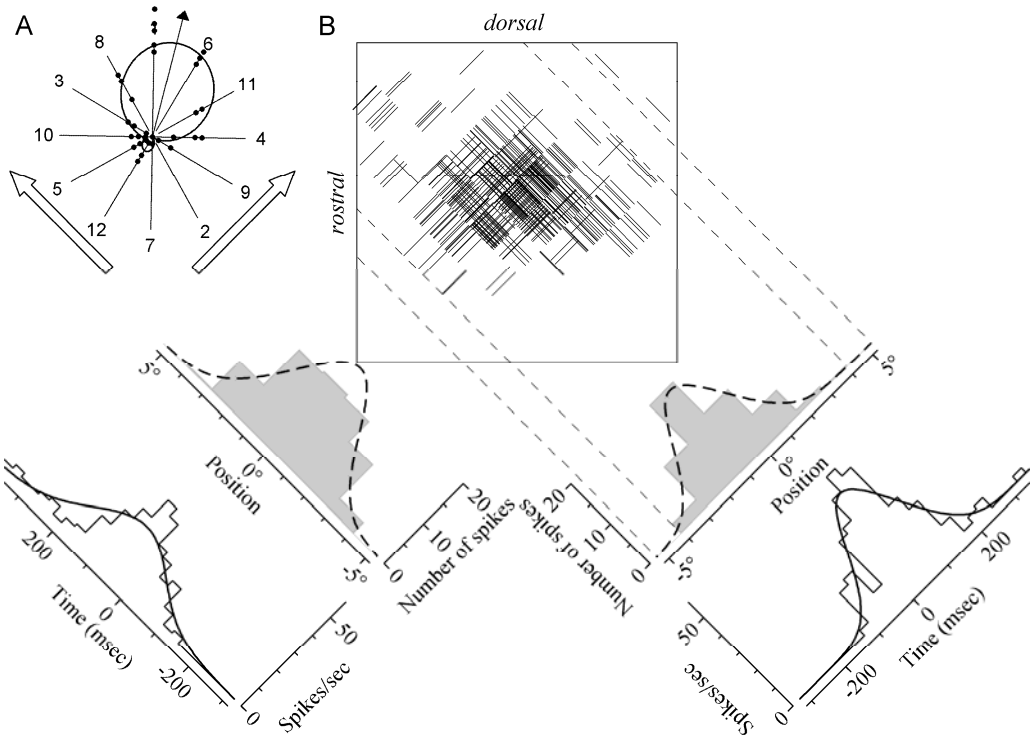

Fig. 3. ERF tracing by small contrast spot moving along several parallel tracks in the stimulation area (Method 3). (A) An example of polar diagram of an ON DS unit, selective to ventro-dorsal movement. Display format as in Fig. 1(A). (B) Tracing by small white spot moving along nine parallel tracks against gray background. Tracing was accomplished in each of the two mutually orthogonal directions, marked by open arrows in Fig. 3(A). Velocity of spot movement was 16.5°/sec. Three stimulus runs were applied in each of the nine tracks. Positions of the spot leading edges at the moments of spike appearance are marked by dashes inside square stimulation area. Bar histograms (shown in gray) present calculated number of spikes along parallel tracks for each of directions. Thin interrupted lines mark marginal tracks for the right histogram. Dashed Gaussian curves were calculated from histogram mean *(x)* and σ-values for both directions. Post-stimulus histograms (presented bellow gray histograms) show spike distribution in the response evoked by stimulus movement from the orthogonal direction. Solid Gaussian curves in Fig. 3(B) were calculated from the means and standard deviations of the post-stimulus histograms.

distribution, estimated on the basis of cell responses along tracks for 77 DS GCs (45 ON cells and 32 OFF cells) is given in the histogram (Fig. 4(A)). The mean value of the ERF diameter, calculated for all cells made 4.3 ± 1.0°.

Method 3 allows evaluation of the ERF diameter on the basis of the spike train duration. Cell responses to stimuli along the tracks (bar histograms in Fig. 3(B)) and the PSH of the spike train, evoked by spot movement over the ERF in the orthogonal direction, represent two different evaluations of the ERF extension in the same dimension. PSHs for each of the two directions derived from the spike train duration are shown by thin stepped lines below the bar histograms (Fig. 3(B)). As before, the ERF extensions can be estimated for each of the directions separately, on the basis of calculated σ-values for the PSHs. A geometric mean of these values was considered as the final estimate of the ERF size.

As one can see from Fig. 3(B), the ERF areas determined on the basis of the PSHs (solid Gaussians) were displaced distally with respect to the ERF area estimated by

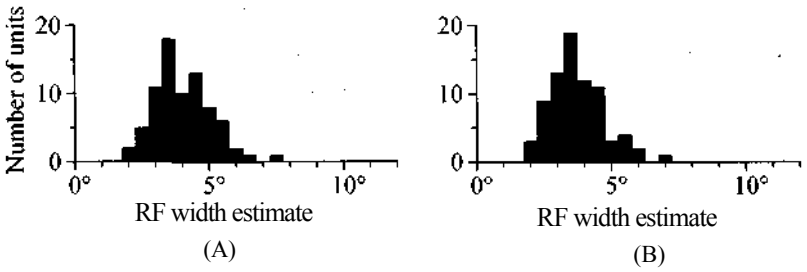

Fig. 4. Histograms showing distribution of the ERF sizes, evaluated by Method 3 for 77 cells. (A) Histogram showing distribution of the ERF sizes, estimated by tracing of ERF area with small contrast spot moving along several parallel tracks in the stimulation area. (B) Histogram showing distribution of the ERF sizes, estimated from the duration of spike train evoked by small contrast spot moving across stimulation area.

the traces (dashed Gaussians). This displacement is a consequence of the fact that spikes, in response to movement of spots, arose with some delay. So, the value of this delay can be determined by the displacement. The mean delay value calculated for the same set of 77 cells was approximately 50 ms. However, irrespective of the delay, the ERF size evaluated on the basis of the spike train duration did not significantly differ from the ERF size estimated on the basis of the cell response along tracks. Histogram of ERF size distribution, estimated on the basis of the spike train duration for 77 cells is shown in Fig. 4(B). The mean ERF size value is 4.0 ± 1.0°. No significant differences in ERF sizes between different types of DS GCs were found.

3.4. *Canonical method of the RF mapping with a flickering spot (Method 4)*

Since the DS units also respond to small stationary flashing spot, there is a possibility of using spots flashed on and off as the stimuli for the ERF mapping. For the DS GCs of the ON-type those were light spots against dark background, while for the DS GCs of the OFF-type the stimuli were dark spots against light background. The spots were flashed on and off sequentially in nodes of square grid in a quasi-random order. Number of spikes evoked by each sequential turning on and off the spot was counted. Since a stationary spot is not an adequate stimulus for the DS units, the number of spikes recorded usually was much lower than in the procedures in which the moving stimuli were applied (see Methods 1, 2, 3). For this reason, each trial was repeated six times. Stimulation was always initiated in the central spot. At the end of the procedure, stimulation was repeated at the central position in order to check unit response level.

Results of the experiment made on the OFF caudo-rostral unit are shown in Fig. 5(B). The area of stimulation was divided into 49 small squares (spots) with slightly greater than 1° in size. Cell responses over the entire stimulation area, measured by this method, are represented in the form of topographic map (see the scale at the bottom of Fig. 5). The extension (length and width) and orientation of

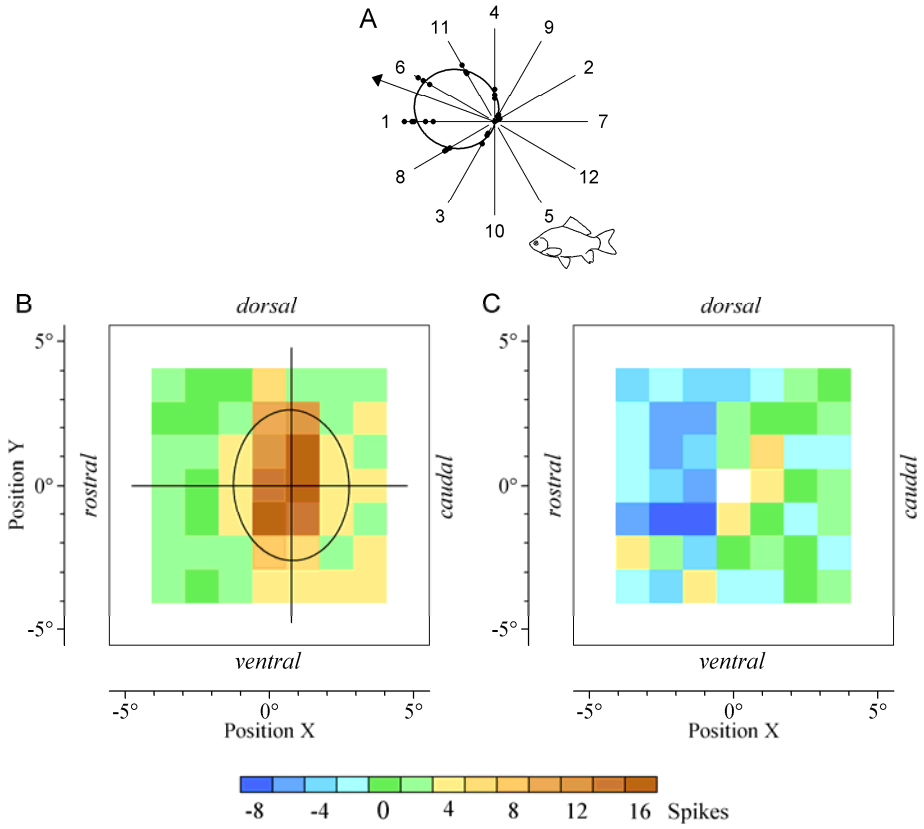

Fig. 5. Canonical method of the ERF mapping with a flashing spots (Method 4). (A) An example of polar diagram of an OFF DS unit, selective to caudo-rostral movement. Display format as in Fig. 1(A). (B) Cell responsiveness across the stimulation area, recorded by ERF mapping with one flashing black spots against light background. Flashing spots were presented six times at each position. Number of spikes was counted after each turning on of the spot. Cell responses over the entire stimulation area, measured by this method, are represented in the form of topographic map (see the scale at the bottom of Fig. 5). The major and minor axes of the ERF were evaluated according to the two-dimensional equivalent of the standard deviation for this data set. The ellipse, constructed on the basis of evaluated ERF axes, presents an estimate of the ERF area. (C) Lateral interactions in the RF of the same OFF caudo-rostral DS unit studied by two flashing spots. The influence of the second spot (located at different position in the stimulation area) on the central one was determined by the difference between mean number of spikes in response to simultaneous stimulation of two spots and mean number of spikes in response to central stimulus alone. The differences were mapped considering the position of the second spot.

the ERF were evaluated according to the two-dimensional equivalent of the standard deviation for this data set. On the basis of estimated extension of the two principal axes of the ERF an ellipse was constructed (see Fig. 5(B)). Such an ellipse was considered to be an estimate of the ERF area, its diameter being evaluated as a geometric mean of its length and width.

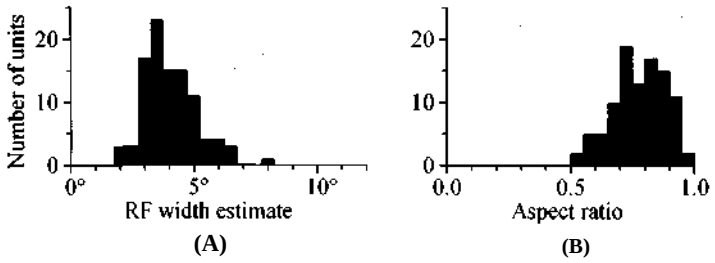

Fig. 6. Distribution of the ERF sizes (A), evaluated by Method 4 for 99 cells, and the distribution of aspect ratios (ratios of minor to major axes of the ERFs) for the same cells (B).

Only stable single unit records from the DS units were used for this analysis. Spontaneous activity was not observed in the cells analyzed. Histogram of ERF size distribution is represented in the Fig. 6(A), estimated for 99 DS units (73 ON units and 26 OFF units) by means of this method. The ERF sizes, estimated on the basis of the geometric mean of the length of the major and minor axes of the ellipse, varied from 1.8° to 7°, with the mean value of 4.3 ± 1.1°.

The oblongness of a cell ERF was estimated according to the ratio between the minor and major axes of a certain ERF (aspect ratio). Distribution of the aspect ratios for these 99 DS units is shown in Fig. 6(B). Mean aspect ratio calculated for all of the cells was 0.8 ± 0.11. Thus the ERFs in DS units happened to be ellipsoidal in shape. In the majority of the dorso-ventral and ventro-dorsal units the ERFs were elongated in the horizontal direction (i.e., the direction orthogonal to the preferred one). On the other hand, in the caudo-rostral units, regularity in orientation of the ERFs was not observed. Vertical and horizontal orientations of the ERFs occurred with practically equal frequency among these units.

3.5. *Receptive field structure of DS units*

It was shown that the direction selectivity in the rabbit retinal GCs may be caused by the asymmetric delayed inhibition generated by the stimuli moving in the null direction (see [1,26]). Such physiological mechanism predicts that an inhibitory area must be displaced in the preferred direction with respect to the ERF. A special experimental procedure was designed in order to check this prediction. By means of this procedure lateral interactions in the RF of the DS units were analyzed. The method permitted analysis of interaction in the stimulation area using two small spots that flashed simultaneously. The stimulation area was divided into small squares, similar to Method 4. At the beginning of the procedure the central flickering spot was presented as a reference stimulus. The number of spikes evoked by each flash of the test stimulus was counted. After six presentations of the reference stimulus, we started to investigate how stimulation of neighboring points of the visual field influenced the reaction in response to stimulation of the central spot, which was made by stimulation with two flashing spots. One of the spots always flashed in

the centre, while the second spot flashed in different positions of the stimulation area in a quasi-random order. Both spots flashed six times simultaneously in each position. The influence of the second spot on the central one was determined by the difference between mean number of spikes in response to stimulation of two spots and mean number of spikes in response to reference stimulus alone. When this value was negative, one could say that there was an inhibitory influence of the second spot. These differences were mapped considering the position of the second flickering spot. Figure 5(C) illustrates results obtained for the same OFF caudo-rostral unit whose ERF, is shown in Fig. 5(B). One can see that an inhibitory (blue) area is adjacent to the preferred side of the ERF. Similar results were obtained for 15 of 26 units analyzed. In 11 of 26 cells the inhibitory area was not detected because of the high loss of cell response level during the procedure.

4. Discussion

In the previous works [18, 19] responses recorded from the *C. gibelio* DS units were attributed to axons of DS GCs projecting to the TO. Responses, similar to these from DS units examined in our work, were recorded in the fish visual nerve fibers on the level of optic chiasm [8, 29] and in the retina [2]. At least one of the possible targets of DS GCs in TO is well known — DS tectal neurons. Responses of DS tectal neurons were regularly recorded at different depths in the TO [18, 19]. The impulses of DS GCs differed from the responses from DS tectal neurons in pattern of the spike train and waveform. Besides, responses of the DS tectal neurons were characterized as ON-OFF responses, whereas DS GCs were separated into ON and OFF center units. In addition, the ERFs of tectal neurons were relatively large, sometimes exceeding the size of the monitor space. On the contrary, ERF sizes of the DS units measured in the present work were much smaller. They were estimated by means of four different methods in the computer-guided experiments. All of the applied methods gave consistent results — mean values of the ERF sizes obtained in the course of these four procedures ranged between 4° and 4.8°. In order to estimate the size of areas in μm on the retinal surface corresponding to these angle values, the geometrical parameters of the fish eye and retina were measured. In a fish of 10 cm long, diameter of lens was 3.2 mm. From this value, according to the ratio of Matthiessen [14] focal distance was calculated and made about 4 mm. On the basis of such focal distance, retinal area corresponding to the ERF size of 4.5° was estimated — it was a rounded area with an approximate diameter of 300 μm.

Since it had been shown that the *C. gibelio* DS GCs used separate ON and OFF pathways [18, 19], it was logical to expect that ON and OFF DS GCs would branch in different sublaminae of the inner plexiform layer (IPL). In the histological study of *C. gibelio* retina, two different morphological GC types were detected [16]. They were both monostratified and branched in different sub-layers of the IPL. Their rounded flat "lacy" dendritic arbors resembled analogous structures of the mammalian fast DS GCs (rabbit [10]; cat [20]; mouse [25]). These rounded flat

dendritic arbors were 200-300 μm in diameter. This diameter corresponds to the ERF size of approximately 300 μm estimated for the fish DS units in the present physiological study. Two types of GCs with the dendritic morphology similar to these described with respect to the GCs of *C. gibelio,* were observed also in zebrafish [13].

According to spectral properties of the *C. gibelio* DS GCs [15] one can conclude that in photopic conditions the DS GCs receive inputs from red sensitive cones mostly, which are principal elements of double-cones. On a flat preparation of the *C. gibelio* retina, one can notice distinguishable areas with regular cone mosaics. According to our measurements, the mean distance between rows of double-cones in these structures was about 15 μm. From this data a total number of red sensitive cones converging on the DS GC can be estimated as 200-300 double-cones per cell.

According to their preferred directions, the *C. gibelio* DS GCs resemble the rabbit's slow ON center DS GCs, characterized by large ERFs. But small ERFs of the fish DS GCs measured in the current study indicate that the fish DS units should be classified as detectors of local motion. Small ERFs were described in the rabbit "fast" ON-OFF DS GCs as well (see review [23]). In contrast to fish DS units, however, these cells preferred four directions separated by about 90°.

In the rabbit retina it was shown that asymmetric delayed inhibition from cholinergic "starburst" amacrine cells produces retinal directional selectivity (see reviews [5, 22]). Results of the present study, obtained from the fish tectum, confirm prediction of the asymmetric delayed inhibition mechanism, i.e., the inhibitory area verges on the ERF side which is more distal relative to the vector indicating preferred direction (see Fig. 5(C)). Inhibitory areas, recorded in the RF peripheries of the fish DS units confirm that the ERF mapping using Method 4 gives valid estimates of the ERF sizes. Since all of the applied methods gave consistent estimates of the ERF sizes (about 300 μm), one can conclude that DS GCs of *C. gibelio,* similarly to the rabbit ON-OFF DS GCs, can be classified as "fast" DS units, and are most likely to be involved in the detection of small objects moving in the surrounding environment.

Acknowledgments

We are grateful to Paul Maximov for the engineering support of the experiments and to Anna Kasparson who provided improvements to our English. We thank Roman Poznanski for his valuable comments and suggestions on the manuscript and the members of our laboratory for many helpful discussions. The study was supported by grants 04-04-49430 and 07-04-00516 from the Russian Foundation for Basic Research.

References

[1] Barlow HB, Levick WR, The mechanism of directionally selective units in the rabbit's retina, *J Physiol (London)* 178:477–504, 1965.

[2] Billota J, Abramov J, Orientation and direction tuning of goldfish ganglion cells, *Visual Neurosci* 2:3–13, 1989.

[3] Chiao CC, Masland RH, Contextual tuning of direction-selective retinal ganglion cells, *Nature Neurosci* 6:1251–1252, 2003.

[4] Cronly-Dillon JR, Units sensitive to direction of movement in goldfish tectum, *Nature* 203:214–215, 1964.

[5] Demb JB, Cellular mechanisms for direction selectivity in the retina, *Neuron* 55:179–186, 2007.

[6] Devries SH, Baylor DA, Mosaic arrangement of ganglion cell receptive fields in rabbit retina, *J Neurophysiol* 78:2048–2060, 1997.

[7] Gaestesland RC, Howland B, Lettvin JY, Pitts WH, Comments on microelectrodes, *Proc IRE* 47:1856–182, 1959.

[8] Jacobson M, Gaze RM, Types of visual response from single units in the optic tectum and optic nerve of the goldfish, *Q J Exp Physiol* 49:199–209, 1964.

[9] Kawasaki M, Aoki K, Visual responses recorded from the optic tectum of the Japanese dace, *Tribolodon hakonensis, J Comp Physiol A* 152:147–153, 1983.

[10] Kittila CA, Massey SC, Pharmacology of directionally selective ganglion cells in the rabbit retina, *J Neurophysiol* 77:675–689, 1997.

[11] Kuffler SW, Discharge patterns and functional organization of the mammalian retina, *J Neurophysiol* 16:37–68, 1953.

[12] Liege B, Galand G, Types of single-unit visual responses in the trout's optic tectum, in Gudikov A (ed.), *Visual Information Processing and Control of Motor Activity,* Bulgarian Academy of Sciences, Sofia, pp. 63–65, 1971.

[13] Mangrum WJ, Dowling JE, Cohen ED, A morphological classification of ganglion cells in the zebrafish retina, *Visual Neurosci* 19:767–779, 2002.

[14] Matthiessen L, Untersuchungen uber den aplanatismus und die periscopie der krystallinsen des fischauges, *Pfluger Arch Ges Physiol* 21:287–307, 1880.

[15] Maximova EM, Govardovskii VI, Maximov PV, Maximov VV, Spectral sensitivity of direction-selective ganglion cells in the fish retina, *Ann NY Acad Sci* 1048:433–434, 2005.

[16] Maximova EM, Levichkina EV, Utina IA, Morphology of putative direction-selective ganglion cells traced with Dii in the fish retina, *Sensory Systems* 20:279–287, 2006 (in Russian).

[17] Maximova EM, Orlov OYu, Dimentnman AM, Investigation of visual system of some marine fishes, *Voprocy Ichtiologii* 11:893–899, 1971 (in Russian).

[18] Maximov VV, Maximova EM, Maximov PV, Direction selectivity in the goldfish tectum revisited, *Ann NY Acad Sci* 1048:198–205, 2005a.

[19] Maximov VV, Maximova EM, Maximov PV, Classification of direction-selective units recorded in the goldfish tectum, *Sensory Systems* 19:322–335, 2005b (in Russian).

[20] O'Brien BJ, Isayama T, Berson DM, Light responses of morphologically identified cat ganglion cells, *Invest Ophtalmol Vis Sci* 40:S815, 1999.

[21] Oyster CW, Barlow HB, Direction-selective units in rabbit retina: Distribution of preferred directions, *Science* 155:841–842, 1967.

[22] Poznanski RR, Biophysical mechanisms and essential topography of directionally selective subunits in rabbit's retina, *J Integr Neurosci* 4:341–361, 2005.

[23] Vaney DI, He S, Taylor WR, Levick WR, Direction-selective ganglion cells in the retina, in Zanker JM, Zeil J (eds.), *Motion Vision: Computational, Neural, and Ecological Constraints,* Springer-Verlag, Berlin, pp. 13–56, 2001.

[24] Wartzok D, Marks WB, Directionally selective visual units recorded in optic tectum of the goldfish, *J Neurophysiol* 36:588–604, 1973.

[25] Weng S, Sun W, He S, Identification of ON-OFF direction-selective ganglion cells in the mouse retina, *J Physiol* 562:915–923, 2005.

[26] Wyatt HJ, Daw NW, Directionally sensitive ganglion cells in the rabbit retina: Specificity for stimulus direction, size, and speed, *J Neurophysiol* 38:623–626, 1975.

[27] Yang G, Masland RH, Direct visualization of the dendritic and receptive fields of directionally selective retinal ganglion cells, *Science* 258:1949–1952, 1992.

[28] Yang G, Masland RH, Receptive fields and dendritic structure of directionally selective retinal ganglion cells, *J Neurosci* 14:5267–5280, 1994.

[29] Zenkin GM, Pigarev IN, Detector properties of the ganglion cells of the pike retina, *Biophysics* 14:722–730, 1969 (in Russian).